

# Dihydrogen Phosphate as a Hydrogen-Bonding Donor Element: Anion Receptors Based on Acylhydrazone

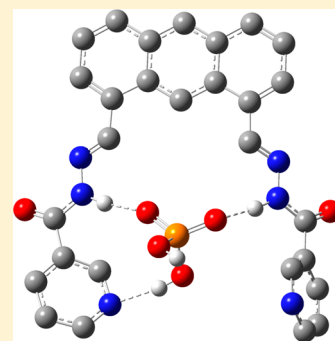
T. Senthil Pandian,<sup>†</sup> Seung Joo Cho,<sup>\*,‡</sup> and Jongmin Kang<sup>\*,†</sup>

<sup>†</sup>Department of Chemistry, Sejong University, Seoul 143-747, South Korea

<sup>‡</sup>Department of Cellular and Molecular Medicine, College of Medicine, Chosun University, 375 Seosuk-dong, Dong-gu, Gwangju 501-759, South Korea

**S** Supporting Information

**ABSTRACT:** Chromogenic anion receptors based on acylhydrazone are designed and synthesized. UV-vis and <sup>1</sup>H NMR titration showed that receptors **1** and **2** are selective receptors for dihydrogen phosphate (H<sub>2</sub>PO<sub>4</sub><sup>-</sup>). Both showed strong association constants with H<sub>2</sub>PO<sub>4</sub><sup>-</sup> even in polar solvents. Receptor **1** was found to recognize H<sub>2</sub>PO<sub>4</sub><sup>-</sup> through three types of hydrogen-bonding (H-bonding) donors: indole N-H, amide N-H, and imine C-H hydrogens. However, receptor **2** seemed to sense H<sub>2</sub>PO<sub>4</sub><sup>-</sup> through two types of H-bonding donors. Despite this seemingly different number of H-bonding elements, the binding constants of receptors **1** and **2** with H<sub>2</sub>PO<sub>4</sub><sup>-</sup> were almost equal. To understand this puzzling result, we investigated the binding poses of complexes using density functional theory. The proposed 2·H<sub>2</sub>PO<sub>4</sub><sup>-</sup> complex structure revealed another possible H-bonding element involving an aromatic nitrogen acting as a H-bonding acceptor. To confirm this, we synthesized receptor **3**, which is devoid of this nitrogen. The binding constant of receptor **3** for H<sub>2</sub>PO<sub>4</sub><sup>-</sup> was 2 orders of magnitude lower than those of receptors **1** and **2**. This decreased binding affinity strongly supports the existence of a N(aromatic)⋯H-O(phosphate) interaction. These results provide a rare opportunity to identify H<sub>2</sub>PO<sub>4</sub><sup>-</sup> acting as a H-bonding donor during an anion-recognition event.

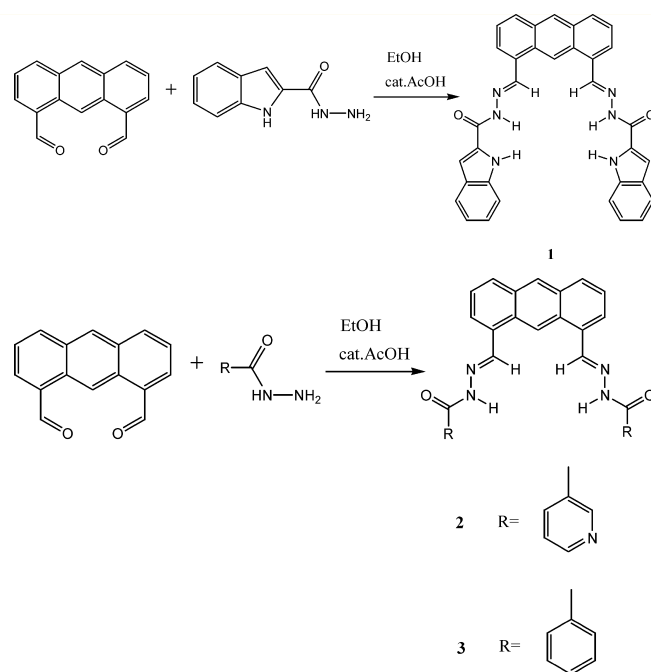


## INTRODUCTION

The design and synthesis of receptors capable of binding and sensing biologically important anions selectively have attracted considerable attention because anions play major roles in the biological, medical, environmental, and chemical fields.<sup>1–12</sup> Of the biologically important anions, phosphorylated species are of considerable interest because they play important roles in a variety of biological processes, such as energy transduction, signal processing, genetic information storage, and membrane transport.<sup>13</sup> Phosphate is an essential component of many chemotherapeutic and antiviral drugs<sup>14–16</sup> as well as being of concern as a pollutant in inland waterways<sup>17</sup> because of the overuse of agricultural fertilizers, whereas pyrophosphate is involved in important anabolic and bioenergetic processes.<sup>18–22</sup> Thus, the importance of the selective detection of phosphorylated biomolecules probably surpasses that of other biologically functional anions.<sup>23–26</sup>

With regard to the design of anion receptors, hydrogen bonds are important anion-recognition elements because of their directionality. Most hydrogen-bonding anion receptors utilize N-H⋯anion or O-H⋯anion hydrogen bonds.<sup>27–29</sup> Rarely, C-H⋯anion hydrogen bonds are also utilized for anion binding<sup>30–38</sup> and play important roles in nature.<sup>39–44</sup>

With these considerations in mind, we designed and synthesized anion receptors **1** and **2**. Receptors **1** and **2** utilize anthracene as a molecular scaffold and acylhydrazone as a hydrogen-bonding moiety. Receptor **1** utilizes three types of H-bonding donors, that is, indole N-H, amide N-H, and imine



C-H bonds, whereas receptor **2** can utilize two types of H-bonding donors, amide N-H and imine C-H bonds.

Received: September 27, 2013

Published: October 30, 2013

**Synthesis.** Receptor **1** was synthesized by reacting anthracene-1,8-dicarbaldehyde<sup>45</sup> and indole-2-acylhydrazide<sup>46</sup> in ethanol using acetic acid as a catalyst at a yield of 74%.

Receptor **2** was synthesized by reacting anthracene-1,8-dicarbaldehyde and nicotino hydrazide<sup>47</sup> in ethanol using acetic acid as a catalyst at a yield of 80%.

Receptor **3** was synthesized by reacting anthracene-1,8-dicarbaldehyde and benzhydrazide in ethanol using acetic acid as a catalyst at a yield of 83%.

## RESULTS AND DISCUSSION

**Interactions with Dihydrogen Phosphate.** The ability of receptor **1** to recognize dihydrogen phosphate was studied in DMSO using UV-vis titration spectra. Upon adding increasing amounts of  $\text{H}_2\text{PO}_4^-$ , moderate increases and decreases in absorption at different wavelengths (Figure 1) and multiple

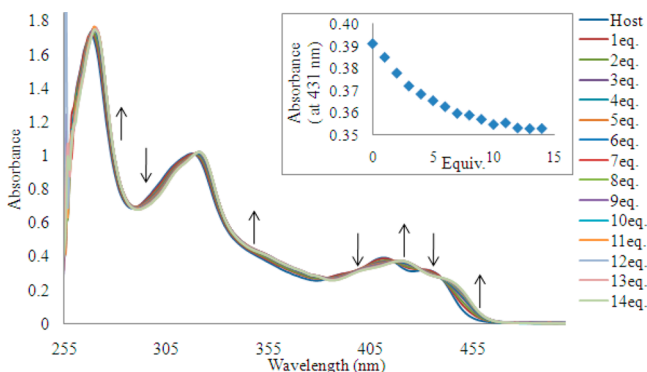


**Figure 1.** Family of spectra recorded over the course of titrating a 20  $\mu\text{M}$  DMSO solution of receptor **1** with increasing amounts of tetrabutylammonium dihydrogen phosphate.

isosbestic points were identified at 268, 288, 318, 382, 416, 429, and 439 nm, suggesting typical hydrogen-bonding complex formation between receptor **1** and dihydrogen phosphate.

Hydrogen-bond formation was confirmed by  $^1\text{H}$  NMR titration. When dihydrogen phosphate was added, two N-H peaks showed intense broadening, and even the imine C-H peak showed line broadening and a downfield shift (Figure 2). We believe that these phenomena were caused by a slow equilibrium between receptor **1** and dihydrogen phosphate as well as the complexation of added dihydrogen phosphate by

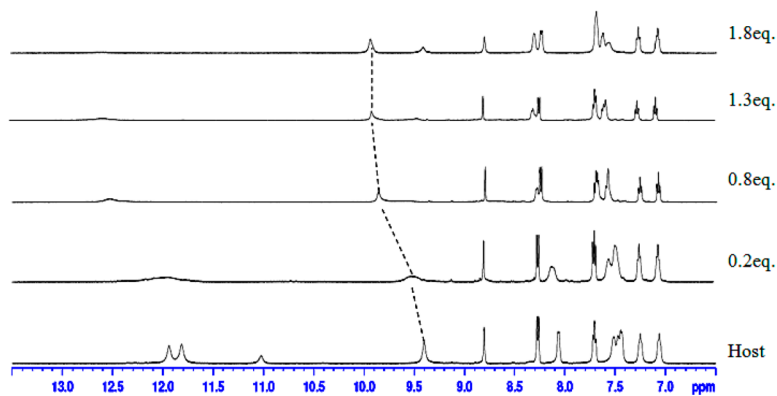


**Figure 2.**  $^1\text{H}$  NMR spectra of 2 mM receptor **1** containing increasing amounts of tetrabutylammonium dihydrogen phosphate (0–1.8 equiv) in  $\text{DMSO-}d_6$ .

receptor **1** through amide N-H, indole N-H, and imine C-H hydrogen-bond formation.

The stoichiometry between receptor **1** and dihydrogen phosphate was determined to be 1:1 using a  $\text{DMSO-}d_6$   $^1\text{H}$  NMR Job plot (Figure 3).

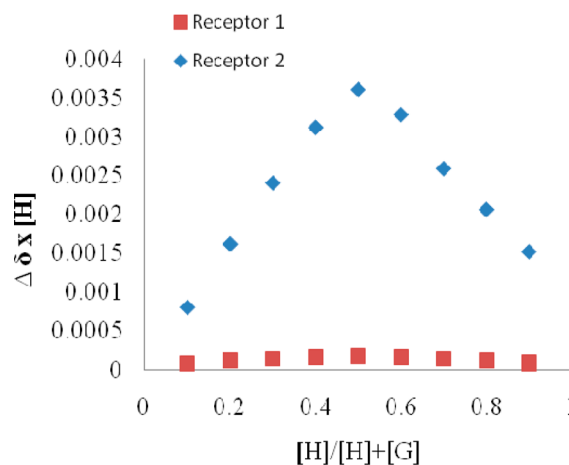


**Figure 3.** Job plots of receptor **1** and **2** with tetrabutylammonium dihydrogen phosphate obtained by  $^1\text{H}$  NMR in  $\text{DMSO-}d_6$ .

The association constant of dihydrogen phosphate for receptor **1** was calculated using a Benesi-Hildebrand plot<sup>48</sup> for UV-vis titration and by analyzing chemical shifts using EQNMR<sup>49</sup> for  $^1\text{H}$  NMR titration. The association constant was calculated to be  $3.2 \times 10^4$  by UV-vis titration and  $3.3 \times 10^4$  by  $^1\text{H}$  NMR titration. To discriminate between H bonding and deprotonation, UV-vis titration of receptor **1** with tetrabutylammonium hydroxide was carried out (Figure 4). Changes in the absorbance spectra in the presence of hydroxide were clearly different from those observed for dihydrogen phosphate. Furthermore, isosbestic points were observed at 282, 321, 355, 398, and 436 nm, which differed from those observed in the presence of dihydrogen phosphate. In addition, receptor UV-vis spectral changes upon adding excessive fluoride were almost identical to those induced by hydroxide.

Figure 5 shows the color change of solutions of receptor **1** after adding various anions in DMSO. Color changes from light green to orange were observed in the presence of hydroxide or fluoride, whereas dihydrogen phosphate did not induce any color change. UV-vis titration results and these color changes

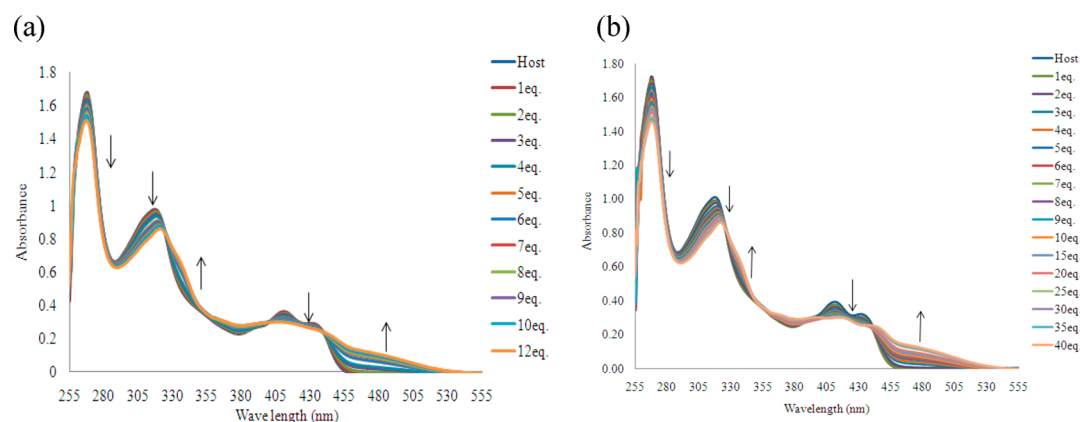


**Figure 4.** Family of spectra recorded over the course of titrating a 20  $\mu\text{M}$  DMSO solution of receptor 1 with increasing amounts of tetrabutylammonium hydroxide (a) and tetrabutylammonium fluoride (b).



**Figure 5.** Color changes of receptor 1 at 100  $\mu\text{M}$  in DMSO when treated with 70 equiv of various anions.

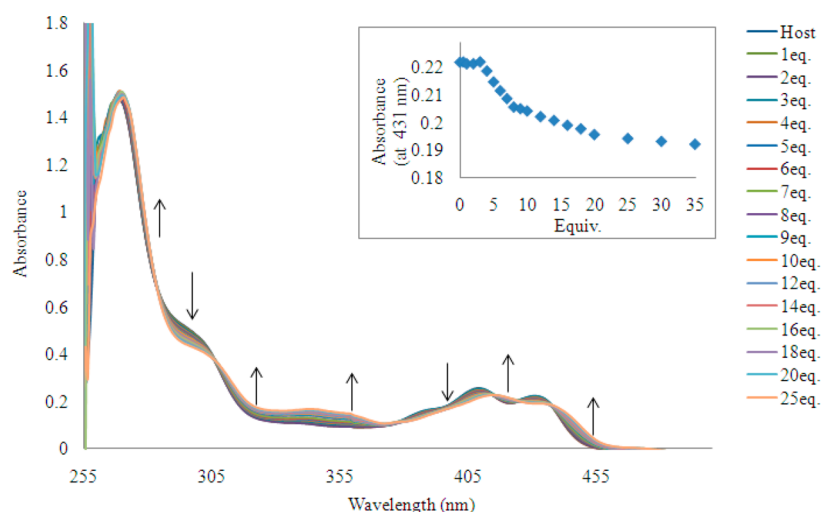


**Figure 6.** Family of spectra recorded over the course of titrating a 20  $\mu\text{M}$  DMSO solution of receptor 2 with increasing amounts of tetrabutylammonium dihydrogen phosphate.

imply a deprotonation event induced by hydroxide and fluoride and hydrogen bonding between dihydrogen phosphate and receptor 1. Pyrophosphate and acetate produced similar deprotonation titration spectra, but the color change caused by pyrophosphate was greater. Because of the small basicity and surface charge density differences between fluoride, acetate, and dihydrogen phosphate, it was difficult to differentiate them

from one another. However, they were able to be differentiated to an extent by considering the different color responses observed. In particular, observed color changes indicated that receptor 1 differentiated hydrogen pyrophosphate and dihydrogen phosphate.

However, the other anions did not induce any color changes, even when added in excess.

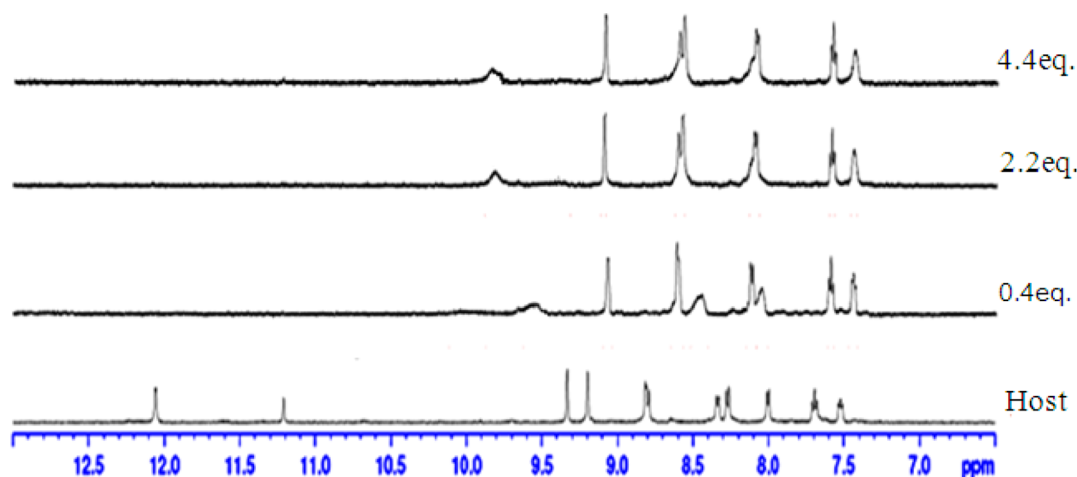


Figure 7.  $^1\text{H}$  NMR spectra of 2 mM receptor 2 with increasing amounts of tetrabutylammonium dihydrogen phosphate (0–4 equiv) in  $\text{DMSO}-d_6$ .

For receptor 2, UV–vis absorption bands at 268, 317, 409, and 431 nm were observed. Upon adding increasing amounts of dihydrogen phosphate, moderate absorption increases and decrease were observed depending on the wavelength (Figure 6).

In addition, multiple isosbestic points emerged at 288, 304, 377, 409, 421, and 431 nm, which suggests that receptor 2 and dihydrogen phosphate formed a typical hydrogen-bonding complex. The  $^1\text{H}$  NMR titration characteristics of receptor 2 in  $\text{DMSO}-d_6$  were similar to those of receptor 1, for example, line broadening of the amide N–H and imine C–H peaks because of slow equilibria were observed on adding dihydrogen phosphate (Figure 7).

A Job plot obtained by  $\text{DMSO}-d_6$   $^1\text{H}$  NMR showed 1:1 stoichiometry, as was observed for receptor 1 (Figure 3). The association constants of dihydrogen phosphate for receptor 2 were  $3.5 \times 10^4$  by UV–vis titration and  $3.6 \times 10^4$  by  $^1\text{H}$  NMR titration.

**Binding Energy Comparison.** These above-mentioned association constants showed that receptors 1 and 2 have similar affinities for dihydrogen phosphate, which was unexpected because receptor 2 seemed to sense  $\text{H}_2\text{PO}_4^-$  through two types of H bonding (amide N–H and imine C–H), whereas receptor 1 appeared to do so through three types of H bonding. Therefore, we decided to investigate the binding poses more accurately using density functional methods. The binding energies of receptors for  $\text{H}_2\text{PO}_4^-$  are listed in Table 1. Experimental binding free energies were obtained from binding constants (UV experiments). Computationally, binding energies were determined using density functional theory. The common hybrid functional of Becke, 3-parameter, Lee–Yang–Parr functional was used along with

Table 1. Comparison of Experimental and Computational Binding Energies with  $\text{H}_2\text{PO}_4^-$ <sup>a</sup>

host	1	2	3
exp (UV)	−6.12 (0.00)	−5.93 (0.19)	−3.39 (2.73)
calc (DFT)	−15.46 (0.00)	−15.20 (0.26)	−12.71 (2.75)

<sup>a</sup>Units are in kcal/mol. Experimental binding energies were derived from UV binding constants. DFT calculations were performed (B3LYP/6-31++G\*\*) using a polarizable continuum model in DMSO. The basis set superposition error was corrected.

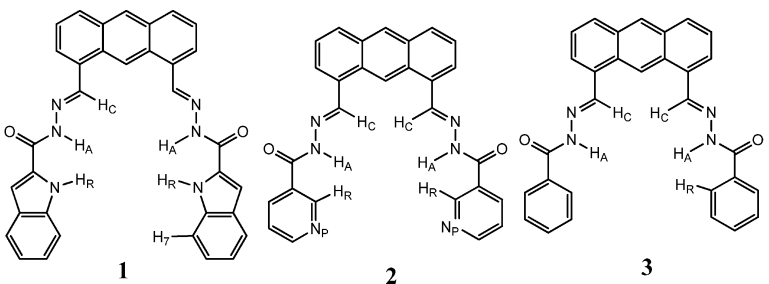
the 6-31+G\* basis set.<sup>50</sup> The solvation effect of DMSO was considered using the PCM (polarizable continuum model).<sup>51</sup>

For complex structures, several geometries were obtained. Here, we chose the lowest-energy structures as representative structures. All geometries of hosts, guest, and complexes were fully optimized without any constraints using stringent optimization criteria. Basis set superposition error corrections were performed.<sup>52</sup> We could not perform second-derivative calculations because of limitations of computational resources, and we assumed that binding free energies (experiment) should correlate with binding energy (calculation) values (Table 2). When experimental and theoretical values were compared, calculated absolute binding energies differed. This was not unexpected because we used crude solvation models for the theoretical calculations and the host- $\text{H}_2\text{PO}_4^-$  complex interactions are very complicated. However, the relative binding energies of hosts (data in parentheses) were similar (differences were less than 0.1 kcal/mol). See the Supporting Information for detailed computational procedures.

**Experimental Confirmation of N(pyridine)⋯H–O–( $\text{H}_2\text{PO}_4^-$ ) H Bonding in  $2 \cdot \text{H}_2\text{PO}_4^-$  Complexes.** The calculated complex structures contained all experimentally observed H-bonding elements (Figure 8). What is remarkable from the binding pose of the  $2 \cdot \text{H}_2\text{PO}_4^-$  complex is the prediction of an additional H-bonding element, that is, N(pyridine)⋯H–O( $\text{H}_2\text{PO}_4^-$ ) H bonding was predicted in the  $2 \cdot \text{H}_2\text{PO}_4^-$  complex (Figure 8, 2).

This additional H bonding would explain why both hosts have similar binding constants. Control experiments were designed and performed to investigate the importance of this H bonding element. Receptor 3, in which the terminal aromatic rings of receptor 2 were changed from pyridine to benzene, was synthesized, and its binding to dihydrogen phosphate under the same conditions was investigated. The binding constant of dihydrogen phosphate for receptor 3 was  $3.1 \times 10^2$  by UV titration. This binding constant is 2 orders of magnitude lower than that of receptor 1 or 2. Accordingly, this substantial lower binding affinity of receptor 3 supports the presence of additional H bonding not observed under the usual experimental conditions.

**Further Inspection of the Binding Poses of Various Complexes.** Figure 8 shows all the possible H-bonding interactions between dihydrogen phosphate and receptors 1, 2, and 3 derived from AIM (atoms in molecules) theory.<sup>53</sup>

Table 2. Geometries and Charges of Hosts and their H<sub>2</sub>PO<sub>4</sub><sup>-</sup> Complexes<sup>a</sup>


The figure shows three chemical structures labeled 1, 2, and 3. Structure 1 is a complex with a fluorenyl-like core and an imine group. Structure 2 is similar but includes a pyridine ring. Structure 3 is a simpler structure with a fluorenyl-like core and an imine group. Below the structures is a table of geometric and charge data for each host and its complex with H<sub>2</sub>PO<sub>4</sub><sup>-</sup>.

host (complex)		1	2	3	1·H <sub>2</sub> PO <sub>4</sub> <sup>-</sup>	2·H <sub>2</sub> PO <sub>4</sub> <sup>-</sup>	3·H <sub>2</sub> PO <sub>4</sub> <sup>-</sup>
Q (H)	H <sub>C</sub>	0.0210	0.0158	0.0159	0.0664	0.0995	0.0995
	H <sub>A</sub>	0.3970	0.3894	0.3915	0.4866	0.5154	0.5064
	H <sub>R</sub>	0.4692	0.1147	0.0152	0.5184	0.0997	0.0923
	H <sub>7</sub> / H <sub>P</sub>	0.0515 (H <sub>7</sub> )			0.0549 (H <sub>7</sub> )		
bond length (X–H) (Å)	H <sub>C</sub> –C	1.0935	1.0926	1.0926	1.0916	1.0918	1.0905
	H <sub>A</sub> –N	1.0186	1.0170	1.0166	1.0300	1.0358	1.0342
	H <sub>R</sub> –R	1.0117	1.0857	1.0858	1.0260	1.0334	1.0850
	H <sub>7</sub> –C/H <sub>P</sub> –O	1.0864 (H <sub>7</sub> –C)			1.0865 (H <sub>7</sub> –C)	0.9869 (H <sub>P</sub> –O)	
	O–H <sub>P</sub> (0.9731)						
distance (H···B) (Å)	H <sub>C</sub> ···O				2.6897	2.5138	2.4006
	H <sub>A</sub> ···O				1.8440	1.8036	1.8311
	H <sub>R</sub> ···O				1.8187	2.6127	2.6111
	H <sub>7</sub> ···O/H <sub>P</sub> ···N <sub>P</sub>				3.7752 (H <sub>7</sub> ···O)	1.9989 (H···N <sub>P</sub> )	
distance (X···B) (Å)	C(imine)···O				3.7083	3.3845	3.2934
	N(amide)···O				2.8932	2.8327	2.8477
	X(ring)···O				2.8236 (N···O)	3.1907 (C···O)	3.3669 (C···O)
	C···O/N <sub>P</sub> ···O				4.7088 (C···O)	2.9731 (N <sub>P</sub> ···O)	
angle (deg)	C–H <sub>C</sub> ···O				131.9	136.2	138.2
	N–H <sub>A</sub> ···O				173.9	171.9	166.8
	R–H <sub>R</sub> ···O				165.5	112.7	126.7
	C–H <sub>7</sub> ···O/N <sub>P</sub> ···H <sub>P</sub> –O				145.2 (C–H <sub>7</sub> ···O)	168.8 (N···H–O)	
ρ(b)	H <sub>C</sub> ···O				0.005999	0.009452	0.012125
	H <sub>A</sub> ···O				0.030615	0.034551	0.033301
	H <sub>R</sub> ···O				0.033707	0.007423	0.010054
	H <sub>7</sub> ···O/H <sub>P</sub> ···N <sub>P</sub>				0.000591 (H <sub>7</sub> ···O)	0.025545 (N <sub>P</sub> ···H)	
∇ <sup>2</sup> ρ(b)	H <sub>C</sub> ···O				0.022615	0.032983	0.040077
	H <sub>A</sub> ···O				0.099765	0.116493	0.108679
	H <sub>R</sub> ···O				0.114372	0.028010	0.036044
	H <sub>7</sub> ···O/H <sub>P</sub> ···N <sub>P</sub>				0.002454 (H <sub>7</sub> ···O)	0.075499 (N <sub>P</sub> ···H)	

<sup>a</sup>Q is the partial atomic charge derived using AIM theory. Distances are in angstroms (Å), angles are in degrees (°). ρ(b) is the electron density at the bond critical point (BCP). ∇<sup>2</sup>ρ(b) is Laplacian electron density at BCP. When two equivalent values were obtained, average values are listed. For example, H<sub>A</sub>···O distances are all average values. H<sub>C</sub> = imine hydrogen attached to the adjacent carbon, H<sub>A</sub> = amide, and H<sub>R</sub> = 6-member aromatic rings. These hydrogens in all hosts appeared to be important for H<sub>2</sub>PO<sub>4</sub><sup>-</sup> recognition. For host 2, additional hydrogen bonding between pyridine nitrogen (N<sub>P</sub>) and a phosphoric hydrogen (H<sub>P</sub>) appeared important, as shown in Figure 8.

AIMALL (Version 13.05.06)<sup>54</sup> was used to study H-bonding interactions. The green dots in the figure signify bond critical points (BCPs). To form a hydrogen bond, a green dot should connect directly to the pair of atoms (H-bonding acceptor and donor atoms) along the path defined by the electron density gradient. This is one of the most important criteria when examining intermolecular interactions. Using this criterion, the number of possible H-bonding interactions between hosts and H<sub>2</sub>PO<sub>4</sub><sup>-</sup> were 6, 7, and 5 for receptors 1, 2, and 3, respectively, as indicated by either dashed or dotted lines in Figure 8 (dashed lines signify stronger interactions). In Table 2, hydrogen atoms involved in H bonding are denoted as H<sub>C</sub>, H<sub>A</sub>, H<sub>R</sub>, and H<sub>7</sub>, and the pyridine nitrogen of host 2 is denoted as N<sub>P</sub>. Relevant physical parameters involving host–guest interactions are listed. Hydrogen bonding is mostly denoted as

X–H···B, where X–H is a H-bonding donor and B, an acceptor. Usually, the X–H bond length in X–H···B is larger than that of corresponding free X–H bond. However, from the bond lengths of X–H in Table 2, this tendency was not clear, presumably because of the complexity associated with multiple host–guest interactions. For N–H···O and N<sub>P</sub>···H<sub>P</sub>–O type interactions, bond lengths were elongated by >0.1 Å, whereas for C–H···O type interactions, bond lengths were slightly reduced by 0.02–0.05 Å. As the distance (H···B) between donor and acceptor atoms reduces, the interaction intensifies, and the angle (X–H···B) approaches a straight line. In this regard, H-bonding interactions involving N–H<sub>A</sub>···O appeared strong for all three hosts.

In addition, N–H<sub>R</sub>···O in host 1 and N<sub>P</sub>···H–O in host 2 also appeared strong. Interestingly, hydrogen-bonding partners



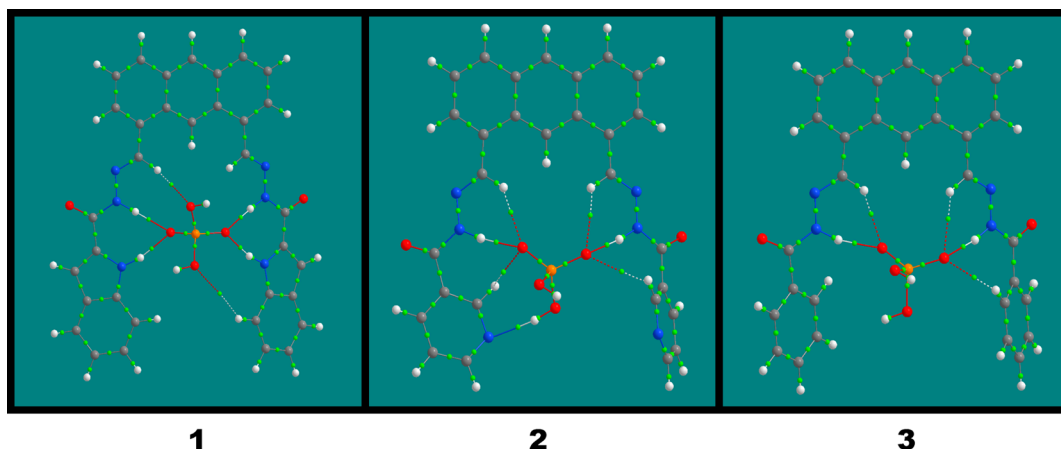


**Figure 8.** Detailed description of H-bonding interactions between receptors **1** and **2** and  $\text{H}_2\text{PO}_4^-$  using AIM theory (AIMALL program). Green dots indicate bond-critical points. Solid lines show strong interactions, and dotted lines show weak interactions. See Table 2 for H-bonding notations.

because of the  $\text{C}-\text{H}\cdots\text{O}$  interaction were positioned farther apart than those involved in heteroatom (N) interactions. This is especially the case for  $\text{C}-\text{H}_7\cdots\text{O}$  in host **1**. The distance between heavy atoms ( $\text{C}\cdots\text{O}$ ) was 4.7 Å, which is close to the upper limit for H bonding. Because host structures are rather rigid and interaction elements are not independent of one another, geometric considerations alone would not be sufficient to determine the relative strengths of H bonding. Therefore, we also considered electronic properties. Another common feature of H bonding is the depletion of electron density around the central H atom. This was found to be the case for all interactions in Figure 8 except for  $\text{H}_R$  in host **2**, where the partial atomic charge was slightly increased by 0.015, which could be caused by the fact that the interaction angle was  $113^\circ$ . All Laplacian values [ $\nabla^2\rho(\text{b})$ ] at BCPs (bond critical points) satisfy the criterion for typical H bonding, that is, they must be positive. One of the most reliable criteria for accessing the strength of H bonding is electron density at the BCP.<sup>55</sup> As listed in Table 2,  $\rho(\text{b})$ s for  $\text{N}-\text{H}\cdots\text{O}$  and  $\text{N}_p\cdots\text{H}_p-\text{O}$  were  $>0.030$ , indicating strong interactions. Other interaction elements were of the  $\text{C}-\text{H}\cdots\text{O}$  type, which has much lower  $\rho(\text{b})$  values (0.007–0.012). For  $\text{C}-\text{H}_7\cdots\text{O}$ ,  $\rho(\text{b})$  was very small (0.000591). Tang et al. suggested that the typical range of  $\rho(\text{b})$  for  $\text{C}-\text{H}$  H bonding is 0.002–0.034 in au.<sup>56</sup> For the  $\text{C}-\text{H}\cdots\text{O}$  interaction, these values were much lower but nevertheless lie within the acceptable range. Accordingly to this criterion, the  $\text{C}-\text{H}_7\cdots\text{O}$  interaction was not classifiable as H bonding. This interaction element should be insignificant. Optimized complex structures are listed in the Supporting Information.

In summary,  $\text{N}-\text{H}\cdots\text{O}$  and  $\text{N}_p\cdots\text{H}_p-\text{O}$  type H bonding appears to be the most significant, whereas  $\text{C}-\text{H}\cdots\text{O}$  H bonding would also participate in molecular recognition. Although the contributions would be insignificant, the  $\text{C}-\text{H}_R\cdots\text{O}$  and  $\text{C}-\text{H}_7\cdots\text{O}$  H bonding would contribute to guest sensing.

## CONCLUSIONS

UV–vis and  $^1\text{H}$  NMR titration showed that receptors **1** and **2** are selective receptors for dihydrogen phosphate. Both receptors showed strong association constants for dihydrogen phosphate, even in polar solvents such as DMSO. In DMSO, dihydrogen phosphate was complexed by receptor **1** via three types of H bonding involving amide  $\text{N}-\text{H}$ , indole  $\text{N}-\text{H}$ , and imine  $\text{C}-\text{H}$ . However, only two types of H bonding were

expected for receptor **2**, namely, amide  $\text{N}-\text{H}$  and imine  $\text{C}-\text{H}$ . Because indole  $\text{N}-\text{H}$  is believed to be a strong H-bonding element, similar binding constants were not anticipated for receptors **1** and **2**. However, theoretical calculations led to the identification of an additional H bonding element. Our findings indicate that the nitrogen atom in the aromatic ring of host **2** appeared to participate in H bonding with the OH of dihydrogen phosphate. This bonding would also explain similar affinities of host **1** and **2** for  $\text{H}_2\text{PO}_4^-$ .  $\text{N}-\text{H}\cdots\text{O}$  and  $\text{N}_p\cdots\text{H}_p-\text{O}$  type H bonding seem to contribute the most to binding, whereas  $\text{C}-\text{H}\cdots\text{O}$  H bonding appears to participate in molecular recognition. In addition, receptor **1** proved to be an effective colorimetric receptor. Fluoride, acetate, pyrophosphate, and dihydrogen phosphate were successfully differentiated by simply adding receptor **1** to their solutions.

## EXPERIMENTAL SECTION

**Receptor 1.** Anthracene-1,8-dicarbaldehyde (70 mg, 0.3 mmol), indole-2-carbohydrazide (107 mg, 0.6 mmol), and three drops of acetic acid were dissolved in 25 mL of ethanol. The mixed solution was heated to reflux overnight and then cooled to room temperature. The formed precipitate was filtered off and washed with ethanol to afford 120 mg (74%) of receptor **1**.  $^1\text{H}$  NMR (500 MHz,  $\text{DMSO}-d_6$ )  $\delta$  11.93 (s, 2H), 11.82 (s, 2H), 11.01 (s, 1H), 9.38 (s, 2H), 8.77 (s, 1H), 8.25 (d,  $J = 8.5$ , 2H), 8.05 (d,  $J = 6.1$ , 2H), 7.69 (t,  $J = 7.6$ , 2H), 7.47 (br, 6H), 7.26 (t,  $J = 6.6$ , 2H), 7.07 (t,  $J = 6.7$ , 2H).  $^{13}\text{C}$  NMR (500 MHz,  $\text{DMSO}-d_6$ )  $\delta$  158.2, 146.9, 136.9, 131.3, 130.5, 130.0, 128.7, 127.9, 127.6, 127.0, 125.7, 123.9, 121.8, 121.3, 120.0, 112.4, 104.4. HRMS (FAB, double focusing mass sector) calcd for  $\text{C}_{34}\text{H}_{25}\text{N}_6\text{O}_2$  [ $\text{M} + \text{H}$ ] $^+$ , 549.2039; found, 549.2039.

**Receptor 2.** Anthracene-1,8-dicarbaldehyde (62 mg, 0.264 mmol), nicotinic hydrazide (72 mg, 0.529 mmol), and three drops of acetic acid were dissolved in 25 mL of ethanol. The mixed solution was heated to reflux overnight and then cooled to room temperature. The formed precipitate was filtered off and washed with ethanol to afford 100 mg (80%) of receptor **2**.  $^1\text{H}$  NMR (500 MHz,  $\text{DMSO}-d_6$ )  $\delta$  12.07 (s, 2H), 11.21 (s, 1H), 9.33 (s, 2H), 9.19 (s, 2H), 8.81 (d,  $J = 3.7$ , 2H), 8.79 (s, 1H), 8.34 (d,  $J = 7.8$ , 2H), 8.27 (d,  $J = 8.7$ , 2H), 8.0 (d,  $J = 6.9$ , 2H), 7.69 (t,  $J = 7.6$ , 2H), 7.52 (t,  $J = 6.1$ , 2H).  $^{13}\text{C}$  NMR (500 MHz,  $\text{DMSO}-d_6$ )  $\delta$  162.5, 152.9, 149.3, 149.2, 135.8, 131.8, 131.3, 130.3, 129.5, 129.2, 128.1, 126.1, 124.0, 122.5. HRMS (FAB, double focusing mass sector) calcd for  $\text{C}_{28}\text{H}_{21}\text{N}_6\text{O}_2$  [ $\text{M} + \text{H}$ ] $^+$ , 473.1726; found, 473.1725.

**Receptor 3.** Anthracene-1,8-dicarbaldehyde (60 mg, 0.256 mmol), benzhydrazide (71 mg, 0.525 mmol), and three drops of acetic acid were dissolved in 25 mL of ethanol. The mixed solution was heated to reflux overnight and then cooled to room temperature. The formed

precipitate was filtered off and washed with ethanol to afford 100 mg (83%) of receptor 3.  $^1\text{H}$  NMR (500 MHz, DMSO- $d_6$ )  $\delta$  11.92 (s, 2H), 11.31 (s, 1H), 9.37 (s, 2H), 8.76 (s, 1H), 8.25 (d,  $J$  = 8.5, 2H), 8.02 (d,  $J$  = 7.6, 2H), 8.0 (d,  $J$  = 6.9, 4H), 7.69 (m, 4H), 7.50 (t,  $J$  = 7.5, 4H).  $^{13}\text{C}$  NMR (500 MHz, DMSO- $d_6$ )  $\delta$  163.3, 147.6, 133.1, 131.3, 131.0, 130.1, 129.8, 128.4, 128.0, 127.3, 126.9, 125.2, 121.8. HRMS (FAB, double focusing mass sector) calcd for  $\text{C}_{30}\text{H}_{23}\text{N}_4\text{O}_2$  [ $\text{M} + \text{H}$ ] $^+$ , 471.1821; found, 471.1821.

## ■ ASSOCIATED CONTENT

### ■ Supporting Information

Binding energy calculations, coordinates for optimized geometries,  $^1\text{H}$  NMR,  $^{13}\text{C}$  NMR, and HRMS spectra for new compounds 1–3. This material is available free of charge via the Internet at <http://pubs.acs.org>.

## ■ AUTHOR INFORMATION

### Corresponding Authors

\*E-mail: chosj@chosun.ac.kr.

\*E-mail: kangjm@sejong.ac.kr.

### Notes

The authors declare no competing financial interest.

## ■ ACKNOWLEDGMENTS

This research was supported by the Basic Science Research Program of the Korean National Research Foundation funded by the Korean Ministry of Education, Science and Technology (2010-0021333).

## ■ REFERENCES

- (1) Jose, D. A.; Kar, P.; Koley, D.; Ganguly, B. *Inorg. Chem.* **2007**, *46*, 5576.
- (2) Velu, R.; Ramakrishnan, V. T.; Ramamurthy, P. *J. Photochem. Photobiol., A* **2011**, *217*, 313.
- (3) Kim, S.-H.; Hwang, I.-J.; Gwon, S.-Y.; Burkinshaw, S. M.; Son, Y. A. *Dyes Pigm.* **2011**, *88*, 84.
- (4) Yang, W.; Yin, Z.; Li, Z.; He, J.; Cheng, J.-P. *J. Mol. Struct.* **2008**, *889*, 279.
- (5) Sessler, J. L.; Cho, D. G.; Lynch, V. *J. Am. Chem. Soc.* **2006**, *128*, 16518.
- (6) Shao, J.; Yu, X.; Xu, X.; Lin, H.; Cai, Z.; Lin, H. K. *Talanta* **2009**, *79*, 547.
- (7) Yang, Z.; Zhang, K.; Gong, F.; Li, S.; Chen, J.; Ma, J. S.; Sobenina, L. N.; Mikhaleva, A. I.; Trofimov, B. A.; Yang, G. *J. Photochem. Photobiol., A* **2011**, *217*, 29.
- (8) Suksai, C.; Tuntulani, T. *Chem. Soc. Rev.* **2003**, *32*, 192.
- (9) Gunnlaugsson, T.; Glynn, M.; Tocci, G. M.; Kruger, P. E.; Pfeiffer, F. M. *Coord. Chem. Rev.* **2006**, *250*, 3094.
- (10) O'Neil, E. J.; Smith, B. D. *Coord. Chem. Rev.* **2006**, *250*, 3068.
- (11) Beer, P. D.; Bayly, S. R. *Top. Curr. Chem.* **2005**, *255*, 125.
- (12) Martinez-Manez, R.; Sancenon, F. *Chem. Rev.* **2003**, *103*, 4419.
- (13) Sessler, J. L.; Cho, D. G.; Lynch, V. *J. Am. Chem. Soc.* **2006**, *128*, 16518.
- (14) Furman, P. A.; Fyfe, J. A.; St. Clair, M. H.; Weinhold, K.; Rideout, J. L.; Freeman, G. A.; et al. *Proc. Natl. Acad. Sci. U.S.A.* **1986**, *83*, 8333.
- (15) Kral, V.; Sessler, J. L. *Tetrahedron* **1995**, *51*, 539.
- (16) Ojida, A.; Mito-oka, Y.; Sada, K.; Hamachi, I. *J. Am. Chem. Soc.* **2004**, *126*, 2454.
- (17) Gale, P. A. *Chem. Commun.* **2005**, *30*, 3761.
- (18) Mathews, C. K.; van Holde, K. E. *Biochemistry*; Benjamin Cummings Publishing Co., Inc.: Redwood City, CA, 1990.
- (19) Ronaghi, M.; Karamohamed, S.; Pettersson, B.; Uhlen, M.; Nyren, P. *Anal. Biochem.* **1996**, *242*, 84.
- (20) Xu, S.; He, M.; Yu, H.; Cai, X.; Tan, X.; Lu, B.; Shu, B. *Anal. Biochem.* **2001**, *299*, 188.

- (21) Lopacinska, K. D.; Strosznajder, J. B. *J. Physiol. Pharmacol.* **2005**, *56*, 15.
- (22) Kamenetsky, M.; Middelhaufe, S.; M. Bank, E.; Levin, L. R.; Buck, J.; Steegborn, C. *J. Mol. Biol.* **2006**, *362*, 623.
- (23) Lee, G. W.; Singh, N.; Jang, D. O. *Tetrahedron Lett.* **2008**, *49*, 1952.
- (24) Shao, J.; Lin, H.; Shang, X. F.; Chen, H. M.; Lin, H. K. *J. Inclusion Phenom. Macrocyclic Chem.* **2007**, *59*, 371.
- (25) Jimenez Blanco, J. L.; Bootello, P.; Benito, J. M.; Ortiz Mellet, C. J.; Garcia Fernandez, M. *J. Org. Chem.* **2006**, *71*, 5136.
- (26) Jose, D. A.; Mishra, S.; Ghosh, A.; Shrivastav, A.; Mishra, S. K.; Das, A. *Org. Lett.* **2007**, *9*, 1979.
- (27) Llinares, J. M.; Powell, D.; Bowman-James, K. *Coord. Chem. Rev.* **2003**, *240*, 57.
- (28) Bondy, C. R.; Loeb, S. J. *Coord. Chem. Rev.* **2003**, *240*, 77.
- (29) Ilioudis, C. A.; Steed, J. W. *J. Supramol. Chem.* **2001**, *1*, 165.
- (30) In, S.; Cho, S. J.; Lee, K. H.; Kang, J. *Org. Lett.* **2005**, *7*, 3993.
- (31) Castellano, R. K. *Curr. Org. Chem.* **2004**, *8*, 845.
- (32) Ilioudis, C. A.; Tocher, D. A.; Steed, J. W. *J. Am. Chem. Soc.* **2004**, *126*, 12395.
- (33) Turner, D. R.; Spencer, E. C.; Howard, J. A. K.; Tocher, D. A.; Steed, J. W. *Chem. Commun.* **2004**, 1352.
- (34) Chmielewski, M. J.; Charon, M.; Jurczak, J. *Org. Lett.* **2004**, *6*, 3501.
- (35) Kang, S. O.; VanderVelde, D.; Powell, D.; Bowman-James, K. *J. Am. Chem. Soc.* **2004**, *126*, 12272.
- (36) Kwon, J. Y.; Jang, Y. J.; Kim, S. K.; Lee, K.-H.; Kim, J. S.; Yoon, J. *J. Org. Chem.* **2004**, *69*, 5155.
- (37) Costero, A. M.; Banuls, M. J.; Aurell, M. J.; Ward, M. D.; Argent, S. *Tetrahedron* **2004**, *60*, 9471.
- (38) Ghosh, S.; Choudhury, A. R.; Row, T. N. G.; Maitra, U. *Org. Lett.* **2005**, *7*, 1441.
- (39) Metzger, S.; Lippert, B. *J. Am. Chem. Soc.* **1996**, *118*, 12467.
- (40) Auffinger, P.; Louise-May, S.; Westof, E. *J. Am. Chem. Soc.* **1996**, *118*, 1181.
- (41) Desiraju, G. R. *Acc. Chem. Res.* **1991**, *24*, 290.
- (42) Steiner, T.; Saenger, W. *J. Am. Chem. Soc.* **1992**, *114*, 10146.
- (43) Sharma, C. V. K.; Desiraju, G. R. *J. Chem. Soc., Perkin Trans.* **1994**, *2*, 2345.
- (44) Chaney, J. D.; Goss, C. R.; Foltz, K.; Santarsiero, B. D.; Hollingworth, M. D. *J. Am. Chem. Soc.* **1996**, *118*, 9432.
- (45) Iwasawa, T.; Hooley, R. J.; Rebek, J., Jr. *Science* **2007**, *317*, 493.
- (46) Zhao, H.; Burke, T. R., Jr. *Tetrahedron* **1997**, *53*, 4219.
- (47) Khan, K. M.; et al. *Bioorg. Med. Chem.* **2003**, *11*, 1381.
- (48) Benesi, H.; Hildebrand, H. *J. Am. Chem. Soc.* **1949**, *71*, 2703.
- (49) Hynes, M. J. *J. Chem. Soc., Dalton Trans.* **1993**, 311.
- (50) Becke, A. D. *J. Chem. Phys.* **1993**, *98*, 1372.
- (51) Tomasi, J.; Mennucci, B.; Cammi, R. *Chem. Rev.* **2005**, *105*, 2999.
- (52) Simon, S.; Duran, M.; Dannenberg, J. J. *J. Chem. Phys.* **1996**, *105*, 11024.
- (53) Bader, R. F. W. *Acc. Chem. Res.* **1975**, *8*, 34.
- (54) Keith, T. A. AIMAll, version 13.05.06; TK Gristmill Software: Overland Park, KS, 2013.
- (55) Koch, U.; Popelier, L. A. *J. Phys. Chem.* **1995**, *99*, 9747.
- (56) Tang, T. H.; Hu, W. J.; Yan, D. Y.; Cui, Y. P. *J. Mol. Struct.* **1990**, *207*, 319.